Developmental Cell *10*, 57–69, January, 2006 ©2006 Elsevier Inc. DOI 10.1016/j.devcel.2005.12.005

Polycystin-1, STAT6, and P100 Function in a Pathway that Transduces Ciliary Mechanosensation and Is Activated in Polycystic Kidney Disease

Seng Hui Low,[1,2,7] Shivakumar Vasanth,[1,3,7] Claire H. Larson,[4,7] Sambuddho Mukherjee,[1] Nikunj Sharma,[1,5] Michael T. Kinter,[4] Michelle E. Kane,[6] Tomoko Obara,[6] and Thomas Weimbs[1,2,*]

[1] Department of Molecular, Cellular, and Developmental Biology
[2] Neuroscience Research Institute
University of California, Santa Barbara
Santa Barbara, California 93106
[3] School of Biomedical Sciences
Kent State University
Kent, Ohio 44242
[4] Department of Cell Biology
Lerner Research Institute
The Cleveland Clinic
Cleveland, Ohio 44195
[5] Department of Biological, Geological, and Environmental Sciences
Cleveland State University
Cleveland, Ohio 44115
[6] Department of Medicine
MetroHealth Medical Center
Case Western Reserve University
Cleveland, Ohio 44109

Summary

Primary cilia are implicated in the pathogenesis of autosomal-dominant polycystic kidney disease (ADPKD), which results from defects in polycystin-1 (PC1), but the function of PC1 remains poorly understood. Here, we show that PC1 undergoes proteolytic cleavage that results in nuclear translocation of its cytoplasmic tail. The PC1 tail interacts with the transcription factor STAT6 and the coactivator P100, and it stimulates STAT6-dependent gene expression. Under normal conditions, STAT6 localizes to primary cilia of renal epithelial cells. Cessation of apical fluid flow results in nuclear translocation of STAT6. Cyst-lining cells in ADPKD exhibit elevated levels of nuclear STAT6, P100, and the PC1 tail. Exogenous expression of the human PC1 tail results in renal cyst formation in zebrafish embryos. These results identify a novel mechanism of cilia function in the transduction of a mechanical signal to changes of gene expression involving PC1 and show that this pathway is inappropriately activated in ADPKD.

Introduction

Autosomal-dominant polycystic kidney disease (ADPKD) is one of the most common monogenic inherited human diseases (Igarashi and Somlo, 2002; Sutters and Germino, 2003; Torres and Harris, 2003; Wilson, 2004). During disease progression, renal epithelial cells proliferate to form fluid-filled cysts that eventually replace most of the normal renal tissue, resulting in renal failure in 50% of the patients by age 50. Currently, no treatment exists to prevent or slow cyst formation, and most ADPKD patients require renal transplantation or life-long hemodialysis for survival. Mutations in either of two genes, PKD1 and PKD2, are the underlying cause of ADPKD, with PKD1 mutations accounting for over 85% of the cases. The function of the PKD1 gene product, PC1, is poorly understood. PC1 is a large, integral membrane protein with putative extracytoplasmic ligand binding domains, but no physiological ligand has clearly been identified to date. The C-terminal cytoplasmic tail of PC1 has been implicated in signal transduction pathways, including the wnt pathway (Kim et al., 1999b), a pathway leading to AP-1 transcription factor activation (Arnould et al., 1998; Chauvet et al., 2004; Le et al., 2004; Parnell et al., 2002), G protein signaling (Kim et al., 1999a; Parnell et al., 1998), calcium signaling (Nauli et al., 2003; Vandorpe et al., 2001; Xu et al., 2003), and activation of STAT1 (Bhunia et al., 2002). However, it is unknown whether these proposed signaling pathways are altered in ADPKD and if any of them may relate to the altered growth and transport phenotypes of cystic epithelial cells. In order to devise a strategy for therapeutic intervention, it will be critical to identify the function of PC1 that—if defective—leads to renal cystogenesis.

Primary cilia of renal epithelial cells are nonmotile extensions of the apical plasma membranes. Recent evidence suggests that primary cilia in the kidney function as mechanosensors that are sensitive to lumenal fluid flow (Praetorius and Spring, 2001, 2003). Recent results also suggest that PC1 may be involved in mechanosensation (Delmas, 2004; Nauli and Zhou, 2004) because renal epithelial cells derived from PC1 null animals fail to respond to flow-mediated bending of their cilia with an elevation of intracellular calcium (Nauli et al., 2003). PC1 has been detected on primary cilia, and in other cellular locations, but the mechanism of its possible role in mechanotransduction remains unclear (Delmas, 2004). Nevertheless, a link between cilia function and PKD appears very likely because defects in a number of cilia proteins can lead to renal cystic diseases in humans and in animal models (Delmas, 2004; Guay-Woodford, 2003; Zhang et al., 2004). Recently, it was shown that PC1 can undergo proteolysis, which appears to be regulated by lumenal fluid flow (Chauvet et al., 2004). This leads to the generation of a C-terminal fragment that can be detected in nuclei and was reported to play a role in the regulation of the AP-1 pathway (Chauvet et al., 2004) that had previously been implicated as a downstream effector of PC1 (Arnould et al., 1998; Le et al., 2004; Parnell et al., 2002).

We report here the identification of a novel, to our knowledge, signaling pathway that transduces a mechanical signal from primary cilia to changes in gene expression. We found that PC1 undergoes proteolytic cleavage of its cytoplasmic tail, followed by nuclear translocation, and we have identified the transcriptional

*Correspondence: weimbs@lifesci.ucsb.edu
[7] These authors contributed equally to this work.

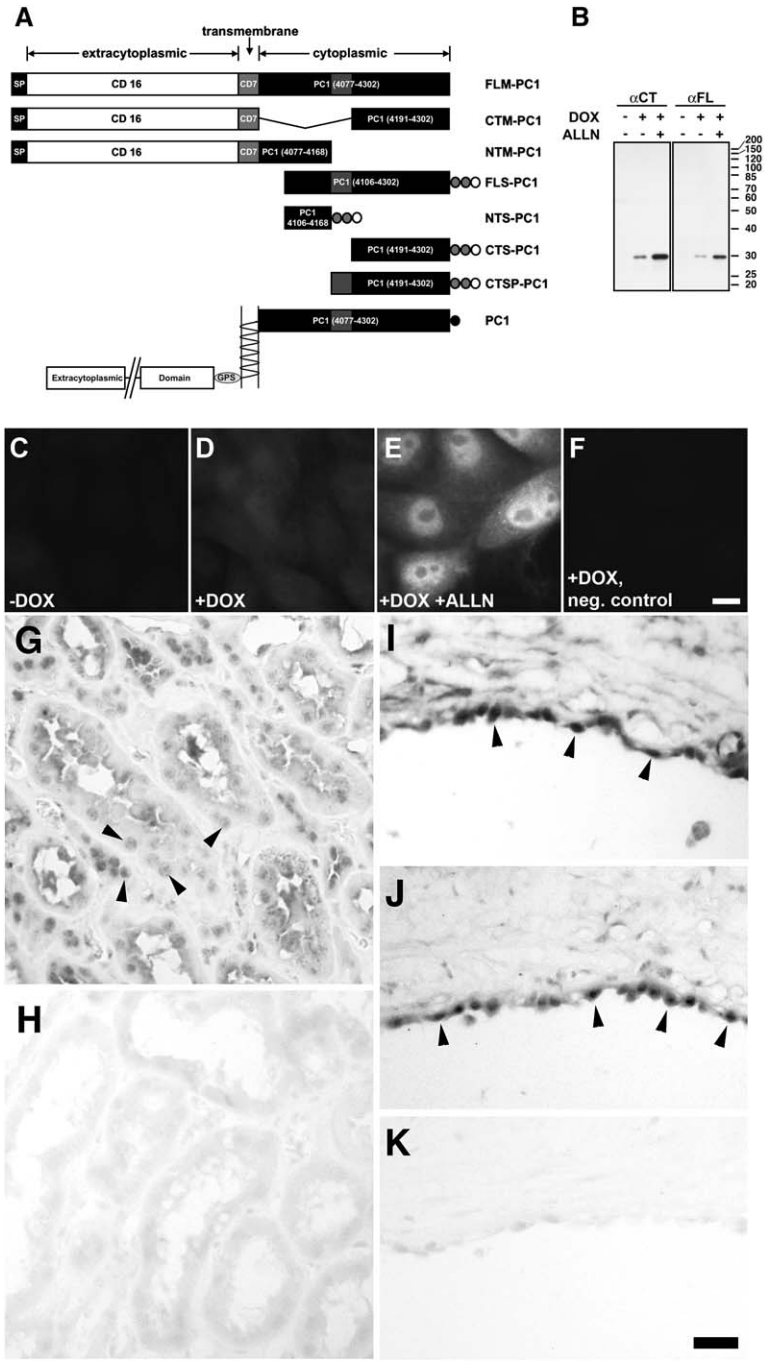

Figure 1. The Cytoplasmic Tail of PC1 Targets to the Nucleus

(A) Expression constructs used in this study. Residue numbers refer to human PC1. Membrane-anchored constructs contain the extracytoplasmic domain and signal peptide (SP) of CD16 and the transmembrane domain of CD7. Epitope tags are: myc (gray circles), His_6 (white circles), and FLAG (black circle).

(B) MDCK cells stably transfected for FLS-PC1 were cultured for 16 hr in the absence or presence of 50 ng/ml DOX and 10 μM ALLN. FLS-PC1 was detected in total cell lysates by Western blot with antibodies against the C-terminal half of the PC1 tail (αCT) or the full-length PC1 tail (αFL). Treatment with ALLN results in significantly elevated levels of FLS-PC1.

(C–E) MDCK cells stably transfected for FLS-PC1 or CTM-PC1 (shown in [F]) were cultured for 16 hr in the absence or presence of 50 ng/ml DOX and 10 μM ALLN. FLS-PC1 is detected by immunofluorescence with an anti-myc epitope tag antibody.

(F) The untagged CTM-PC1 serves as an additional negative control. The scale bar is 10 μm.

(G–K) Immunohistochemical detection of the PC1 tail in (G and H) normal human kidney or (I–K) ADPKD kidney with (G and I) αCT or (J) αFL antibodies. Histological counterstaining was omitted. The arrowheads highlight nuclear signals. (H) and (K) show negative controls with the omission of the primary antibody. For comparison, the immunohistochemistry was carried out side by side, and images were acquired under identical conditions. The scale bar is 20 μm.

machinery that interacts with the PC1 tail and mediates PC1-regulated gene expression. We show that the PC1 tail binds to the sequence-specific transcription factor STAT6 and the coactivator P100, and that it stimulates STAT6-dependent transcription. STAT6 localizes to primary cilia under normal conditions but undergoes nuclear translocation in response to the cessation of apical fluid flow. The PC1/STAT6/P100 pathway is significantly upregulated in cyst-lining epithelial cells in human ADPKD, which suggests its involvement in cellular changes that bring about renal cystogenesis. These results identify a signaling pathway that sheds light on the function of primary cilia and may be a promising target for strategies for therapeutic intervention for ADPKD.

Results

The Cytoplasmic Tail of PC1 Targets to the Nucleus and Is Overexpressed in ADPKD

We initially made the following observation when expressing the C-terminal cytoplasmic tail of PC1 (construct FLS-PC1 in Figure 1A) in the MDCK renal epithelial cell line by stable transfection by using a doxycycline (DOX)-regulatable promotor. DOX induction resulted in very low expression levels in all investigated clones (Figure 1B). Treatment with the proteasome inhibitor ALLN resulted in significantly elevated expression levels, suggesting that FLS-PC1 is subject to rapid proteasomal degradation. Surprisingly, FLS-PC1 localized

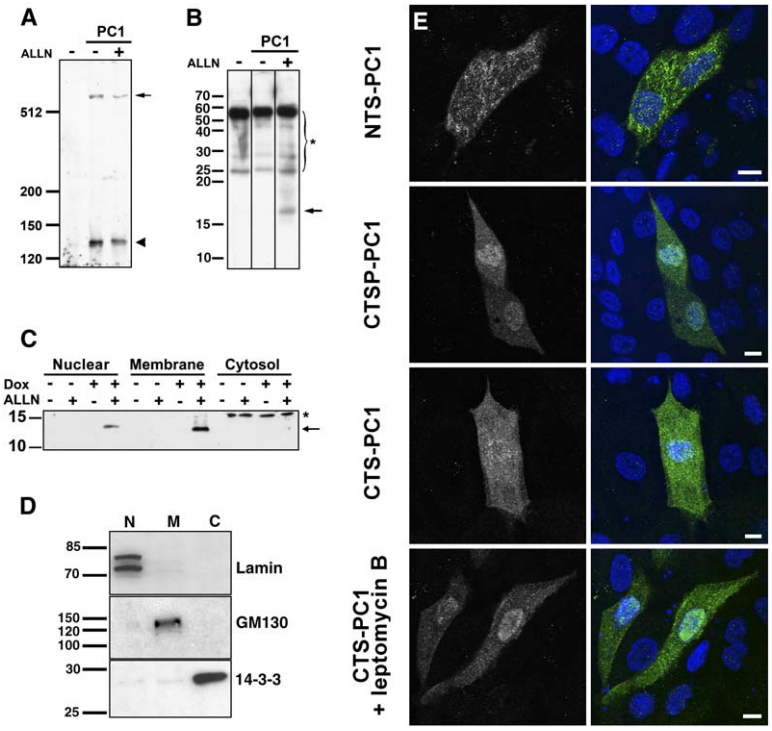

Figure 2. The C-Terminal Half of the PC1 Tail Is Cleaved, Is Released from the Membrane, and Targets to the Nucleus

(A and B) As indicated, COS-7 cells were transiently transfected for C-terminally FLAG-tagged PC1. After treatment for 16 hr in the absence or presence of 10 μM ALLN, cells were lysed and PC1 was immunoprecipitated with the αFL antibody. Immunoprecipitates were separated on a (A) 4% or (B) 15% SDS-PAGE gel and were probed with the αCT antibody in (A). Note the full-length PC1 (arrow in [A]) and the expected ~130 kDa product of cleavage at the GPS domain (arrowhead in [A]). The arrow in (B) indicates a ~17 kDa cleavage product. The asterisk in (B) indicates nonspecific bands including IgG heavy and light chains.

(C) MDCK cells stably transfected for FLM-PC1 were treated for 16 hr with DOX and/or 10 μM ALLN. Cells were fractionated into nuclear, total membrane, and cytosolic fractions by differential centrifugation. The fractions were probed by Western blot with αCT. An ~14 kDa cleavage product is present in fractions of ALLN-treated cells (arrow). The asterisk indicates a nonspecific band.

(D) To control for the purity of fractions in (C), the enrichment of nuclear (lamin), membrane (GM130), and cytoplasmic (14-3-3) markers was tested by Western blot.

(E) MDCK cells were transiently transfected for the indicated PC1 constructs and were immunostained with the αFL antibody (green). Nuclei were stained with DAPI (blue). As indicated, cells were treated with leptomycin B (10 ng/ml) for 3 hr. The scale bars are 10 μm.

preferentially to the nucleoplasm (Figure 1E), suggesting that nuclear targeting of the PC1 tail may have functional significance.

To test whether the cytoplasmic tail of PC1 may also undergo nuclear targeting in vivo, we utilized a polyclonal antibody (termed αFL) against the full-length tail (equivalent to FLS-PC1) and another (termed αCT) against the C-terminal half of the tail (equivalent to CTS-PC1). Immunohistochemistry of normal human kidney with these two antibodies revealed a weak, but reproducible, nuclear signal (Figure 1G). Cyst-lining epithelial cells in renal specimens from ADPKD patients exhibited highly elevated nuclear and cytoplasmic signals (Figures 1I and 1J). These immunosignals were variable between patients and also from cyst to cyst within the same specimen. Whereas some cysts exhibited no detectable signal, the majority were strongly stained.

The C-Terminal Half of the PC1 Tail Is Cleaved and Released from the Membrane

Since PC1 is an integral membrane protein, the finding of nuclear localization suggests that the cytoplasmic tail would have to be released from the rest of the protein by proteolysis prior to nuclear translocation. PC1 can undergo proteolysis at a conserved GPS domain in the N-terminal extracytoplasmic domain (Qian et al., 2002), which generates an ~130 kDa C-terminal fragment that is comprised of all transmembrane domains and the cytoplasmic tail. To test whether an additional cleavage event may release the tail from the membrane, we expressed full-length, C-terminally FLAG-tagged PC1 in COS-7 cells. As shown in Figure 2A, full-length PC1 (arrow) can be detected along with the anticipated product of the cleavage at the GPS domain (arrowhead). Furthermore, a small C-terminal fragment of ~17 kDa can be detected in the presence, but not the absence, of ALLN (Figure 2B, arrow). Since this fragment is detectable with the αCT antibody as well as an antibody against the C-terminal FLAG epitope (data not shown), it must consist of the extreme C terminus of PC1. This result indicates that PC1 not only undergoes cleavage at the GPS domain but that an additional cleavage event can lead to the release of the C-terminal half of the cytoplasmic tail. Whereas the 130 kDa fragment is relatively stable, the 17 kDa fragment appears to undergo rapid proteasomal degradation.

Next, we used MDCK cells that stably express a construct in which the PC1 tail is membrane anchored by fusion to the extracytoplasmic domain of CD16 and the transmembrane domain of CD7 (FLM-PC1, Figure 1A). This leads to the expression of the fusion protein of the expected size of ~75 kDa (data not shown). Treatment with ALLN results in the accumulation of a small fragment of ~14 kDa that reacts with the αCT antibody (Figure 2C, arrow). This fragment can be identified in nuclear and membrane fractions. We estimate that the ~14 kDa fragment that is generated from the FLM-PC1 fusion protein is equivalent to the ~17 kDa

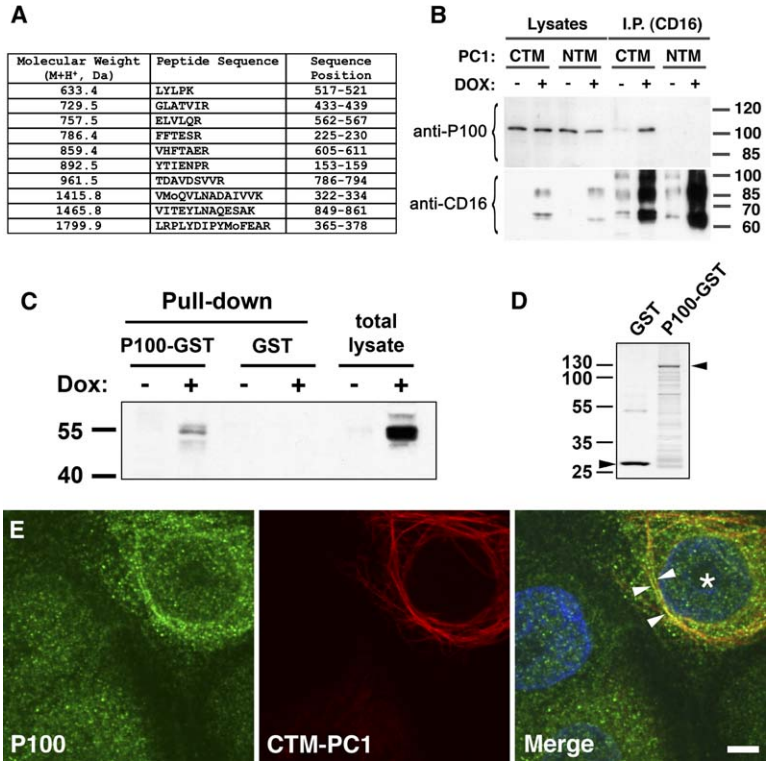

Figure 3. The PC1 Tail Interacts with P100

(A) Sequencing of an ~110 kDa protein band that specifically coimmunoprecipitated with CTM-PC1 expressed in MDCK cells yielded ten peptide sequences belonging to P100 (GenBank accession NM_014390) covering 10% of the sequence. Mo, oxidized methionine.

(B) MDCK cells stably transfected for CTM-PC1 or NTM-PC1 as a control were induced with DOX for 16 hr or left uninduced. PC1 constructs were immunoprecipitated with an antibody against CD16. P100 was detected by Western blot with an antibody against a C-terminal 16 kDa fragment. Note that P100 coprecipitates with CTM-PC1, but not NTM-PC1.

(C) GST and P100-GST fusion proteins were immobilized on glutathione Sepharose and incubated with the lysate of MDCK cells stably expressing CTM-PC1. Bound proteins were analyzed by immunoblot for PC1 with the αCT antibody.

(D) The expression levels of GST and GST-P100 are shown by Coomassie staining in (arrowheads indicate the full-length proteins).

(E) MDCK cells stably transfected for CTM-PC1 were induced with DOX for 16 hr. P100 and CTM-PC1 were detected by confocal immunofluorescence microscopy. The field contains a cell that expresses CTM-PC1 (asterisk), while others do not. The arrowheads highlight colocalization. The scale bar is 5 μm.

fragment generated from full-length PC1 seen in Figure 2B. The size difference is likely due to the additional C-terminal, highly negatively charged FLAG tag of the latter. This result suggests that a cleavage site in the middle of the cytoplasmic tail of PC1 can be recognized and cleaved independent of preceding parts of the molecule.

Nuclear Localization Is Mediated by the C-Terminal Half of the PC1 Tail

To verify that the C-terminal half of the PC1 tail is sufficient for nuclear translocation, we tested three additional constructs (Figure 1A). As shown in Figure 2E, NTS-PC1 mainly localizes to the cytoplasm, whereas both CTS-PC1 and CTSP-PC1 prominently localize to the nucleus in transfected cells. The observed expression levels were consistently lower for CTSP-PC1 than for CTS-PC1, suggesting that the PEST sequence contained in CTSP-PC1 indeed promotes proteasomal degradation. CTS-PC1 appeared to be less concentrated in the nucleus compared to CTSP-PC1. However, treatment with leptomycin B, an inhibitor of nuclear export, resulted in strong nuclear accumulation of CTS-PC1 (Figure 3), suggesting that its initially lower relative nuclear accumulation was due to a saturation effect caused by the higher expression level. These results indicate that nuclear localization is mediated by the C-terminal half of the PC1 tail and suggest that the PC1 tail undergoes nuclear shuttling.

The PC1 Tail Binds to P100

These observations suggested that the cleaved PC1 tail may have a signaling function and may regulate transcription in the nucleus. In order to identify interacting proteins that may mediate this function, we isolated binding proteins by coimmunoprecipitation and protein sequencing by mass spectrometry. CTM-PC1 was expressed in MDCK cells for 16 hr and was immunoprecipitated. Uninduced cells served as negative controls. SDS-PAGE revealed several proteins that specifically bound to CTM-PC1 (data not shown) and were identified by mass spectrometry. A band of ~110 kDa yielded ten peptide identifications belonging to the protein EBNA2 coactivator, also known as P100 (Figure 3A). Immunoblotting with an antibody against P100 verified this identification and showed that P100 coprecipitates with CTM-PC1, but not with NTM-PC1 (Figure 3B). The same band also reacts with an antibody against a different domain of P100 (data not shown). P100 is a ubiquitously expressed transcription factor that was originally identified as a coactivator of the Epstein Barr virus nuclear antigen 2 (Tong et al., 1995).

Next, we generated a recombinant P100-GST fusion protein (Figure 3D) and used it in pull-down experiments with total cell lysates from MDCK cells expressing CTM-PC1 under DOX control. As shown in Figure 3C, CTM-PC1 interacts with P100-GST, but not with GST alone. This confirms the interaction between the PC1 tail and P100 and suggests that it is direct.

As a further test, CTM-PC1 was expressed in subconfluent MDCK cells in which it localizes prominently to the endoplasmic reticulum (Figure 3E). In nontransfected MDCK cells, P100 localizes mainly to the nucleus and diffusely in the cytoplasm. However, in cells that express CTM-PC1 (asterisk), a significant fraction of P100 is retargeted and partially colocalizes with CTM-PC1 (arrowheads), confirming the interaction in vivo. Altogether,

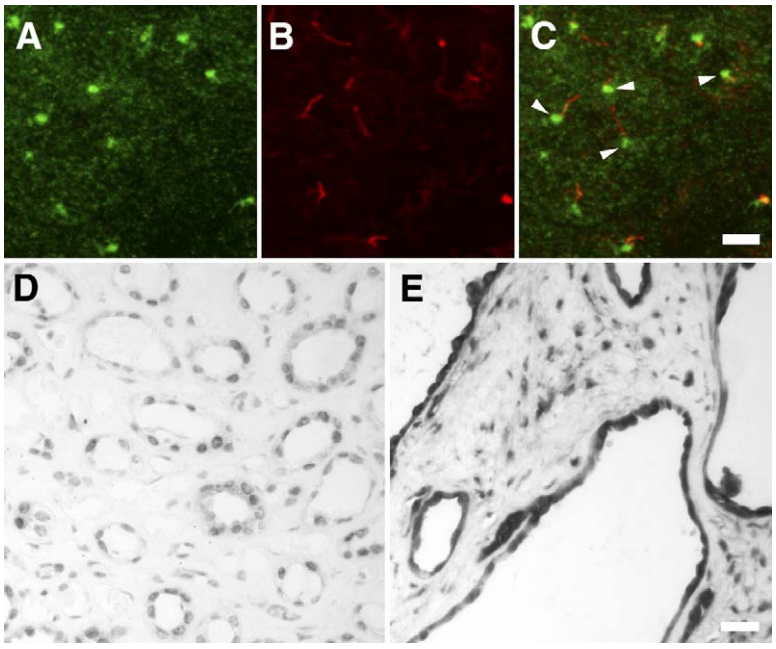

Figure 4. P100 Partially Localizes to Basal Bodies and Cilia and Is Overexpressed in ADPKD

(A–C) MDCK cells were cultured on a filter support for 13 days. P100 (green) and acetylated tubulin (red), a cilia marker, were detected by immunofluorescence microscopy. Shown are projections of confocal optical sections of the apical region of the cells. In addition to nuclear and cytoplasmic staining (data not shown), P100 localizes to the basal bodies underneath the cilia, with a smaller fraction penetrating into the cilia shafts (arrowheads). The scale bar is 5 μm.

(D and E) Immunohistochemistry for P100 in (D) normal human kidney and (E) ADPKD kidney. Histological counterstaining was omitted. For comparison, the immunohistochemistry was carried out side by side, and images were acquired under identical conditions. The scale bar is 20 μm.

these experiments establish that P100 interacts with the C-terminal half of the tail of PC1.

P100 Partially Localizes to the Basal Body and Primary Cilia in Polarized MDCK Cells and Is Overexpressed in ADPKD

P100 has been reported to localize to the nucleoplasm and to cytoplasmic membrane organelles (Broadhurst and Wheeler, 2001; Tong et al., 1995). As shown in Figure 3E, a large fraction of P100 localizes to the nucleus in subconfluent, nonpolarized MDCK cells. To investigate the localization of P100 in fully polarized cells, MDCK cells were cultured on permeable filter supports for 13 days, during which they develop apical primary cilia. Confocal immunofluorescence microscopy with two antibodies against different domains of P100 revealed identical results. In addition to diffuse cytoplasmic and nucleoplasmic staining, a significant fraction of P100 localizes to the basal body from which primary cilia originate, and a minor fraction localizes to the cilia shafts (Figure 4C). PC1 has also been shown to localize to the cilia and the basal bodies of renal epithelial cells (Nauli et al., 2003; Yoder et al., 2002). Therefore, our localization and binding data suggest that a fraction of P100 may exist in a constitutive complex with PC1 on the basal bodies and cilia.

Next, we investigated the expression and localization of P100 in the kidney. As shown in Figure 4D, P100 is expressed in renal epithelial cells and exhibits predominantly nuclear localization in normal human kidney. In ADPKD renal tissue, P100 is overexpressed in the cyst-lining epithelial cells (Figure 4E), which was consistent among all specimens tested. Virtually all cysts exhibited a strong nuclear and cytoplasmic P100 immunosignal, suggesting that the transcriptional activity of P100 is abnormally high in cystic cells. Two different P100 antibodies against different regions of the molecule and another antibody against full-length P100-GST yielded identical results (data not shown).

The PC1 Tail Binds to STAT6 and Stimulates STAT6-Dependent Transcription

Our findings of an interaction between P100 and PC1, and their colocalization at cilia, suggested the possibility that P100 could be involved cilia-mediated mechanosensation. P100 has been shown to bind to the transcription activation domain of STAT6, and to enhance interleukin-4 (IL-4)-induced activation of Igε transcription in human B cells (Yang et al., 2002). P100 appears to function as a bridging protein between the sequence-specific transcription factor STAT6 and the basal transcription machinery (Tong et al., 1995; Yang et al., 2002).

To test whether STAT6 may participate in a signaling pathway involving PC1 and P100, we investigated their potential binding interactions. MDCK cells stably transfected for FLS-PC1 under DOX control were treated with IL-4 or were left untreated, lysed, and subjected to immunoprecipitation with an antibody against STAT6. Figure 5A shows that MDCK cells express endogenous STAT6 and activate it by tyrosine phosphorylation in response to IL-4 treatment. STAT6 specifically precipitates with FLS-PC1 in a DOX-dependent fashion. IL-4 had no apparent effect on the binding to FLS-PC1. Endogenous P100 also coprecipitates with STAT6, and this interaction is also independent of IL-4 (Figure 5A), as previously reported (Yang et al., 2002). These results indicate that the PC1 tail interacts with STAT6, possibly via P100. Neither binding of P100 nor of the PC1 tail requires tyrosine phosphorylation of STAT6, suggesting that these proteins exist in a constitutive complex.

Next, we tested whether the PC1 tail can regulate STAT6-dependent transcription by using a luciferase reporter construct containing five copies of a STAT6 binding element (Haque et al., 1997). Stimulation with a low concentration of IL-4 increases STAT6-dependent luciferase activity 5-fold, as expected (Figure 5B). Coexpression of the FLS-PC1, CTSP-PC1, or CTS-PC1 constructs all resulted in a significant further stimulation of STAT6 activity, whereas the NTS-PC1 construct had

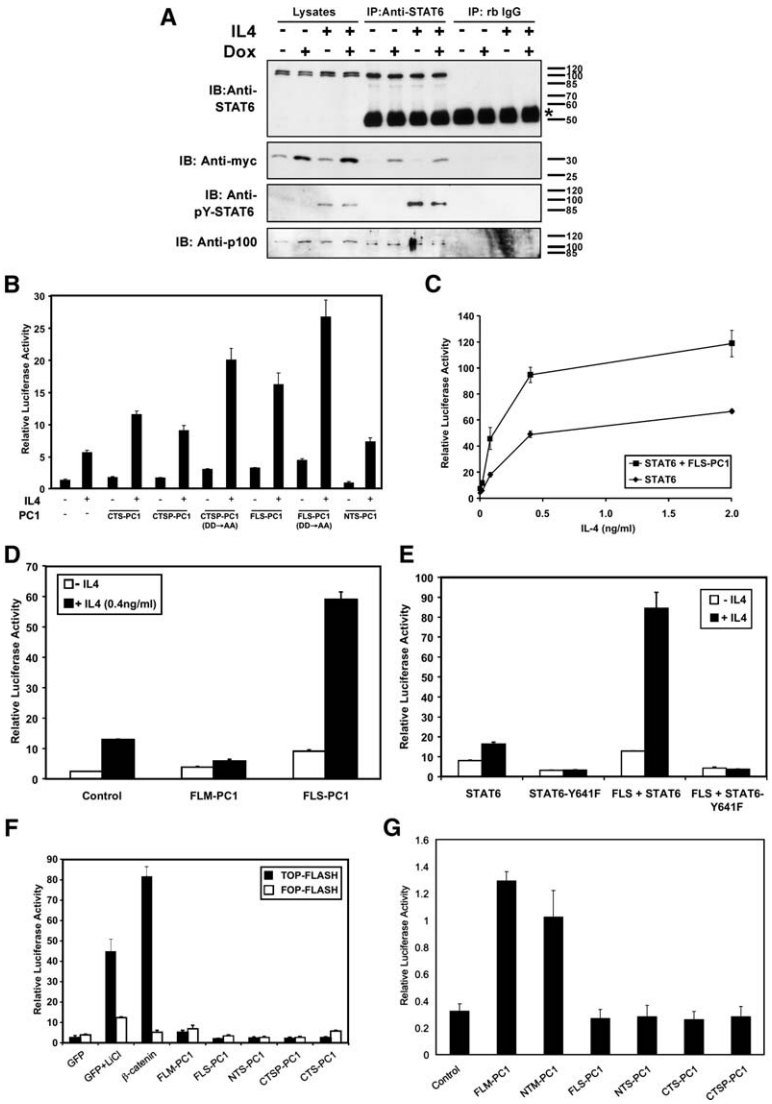

Figure 5. The C-Terminal Half of the PC1 Tail Interacts with STAT6 and Activates STAT6-Dependent Transcription

(A) MDCK cells stably transfected for FLS-PC1 were cultured overnight with ALLN (10 μM) in the presence or absence of DOX (50 ng/ml). Cells were treated with 20 ng/ml canine IL-4 for 30 min where indicated and were lysed for immunoprecipitation with anti-STAT6. Binding proteins were detected with the indicated antibodies. The asterisk denotes the rabbit Ig heavy chain.

(B–G) HEK293T cells were transfected with luciferase reporter constructs containing either (B–E) STAT6, (F) wnt-, or (G) AP-1-responsive promotors along with the indicated PC1 constructs. Reporter assays were carried out 36 hr after transfection. Cells were treated with the indicated concentrations of (C) IL-4 or with (B, D, and E) 0.4 ng/ml IL-4. (F) The wnt reporter contains tandem repeats of TCF/LEF enhancer elements or mutated, inactive elements (TOP- and FOP-FLASH, respectively). Relative luciferase activity represents luciferase units normalized with β-gal activity. Bars + SD are the average of normalized luciferase units from three wells of a 12-well plate, and all experiments were repeated at least three times.

no significant effect. At all concentrations of IL-4 tested, FLS-PC1 further stimulates STAT6 activity (Figure 5C); however, the relative effect is greatest at low IL-4 concentrations. The PC1 tail constructs also stimulate the basal transcriptional activity of STAT6 in the absence of IL-4 by approximately 2-fold (Figure 5B). These results indicate that the C-terminal half of the cytoplasmic tail of PC1 positively regulates STAT6-dependent transcription.

The membrane-anchored PC1 tail (FLS-PC1) does not result in any increase in luciferase activity (Figure 5D), which further suggests that the PC1 tail indeed has to travel to the nucleus to affect STAT6-dependent transcription. We consistently observed a decrease of IL-4-stimulated STAT6 activity upon expression of FLM-PC1 (Figure 5D), which suggests that the membrane-anchored PC1 tail has a dominant-negative function, presumably by membrane sequestration of STAT6 and/or P100.

We mutated two aspartate residues in the PEST motifs of CTSP- and FLS-PC1. As shown in Figure 5B, these DD→AA mutants exhibit increased stimulation of STAT6 activity. This suggests that the stimulatory activity of the PC1 tail is regulated by its degradation, which is mediated by the PEST motif.

Canonical STAT6 activation requires phosphorylation of a critical tyrosine residue (Y641). As shown in Figure 5E, no STAT6-dependent luciferase activity is observed with the Y641F mutant, irrespective of the presence of the PC1 tail, indicating that the regulation by the PC1 tail depends on tyrosine phosphorylation of STAT6.

Altogether, these results show that the C-terminal half of the PC1 tail is capable of interacting with P100 and STAT6, which leads to an enhancement of STAT6-dependent transcription both under basal conditions and after IL-4 induction. The PEST domain in the PC1 tail appears to function in its downregulation.

It has previously been reported that expression of the membrane-anchored constructs FLM-PC1 and CTM-PC1 in transiently transfected HEK293 cells causes activation of the wnt signaling pathway via stabilization of β-catenin (Kim et al., 1999b). To test whether this effect may also involve cleaved, soluble fragments of the PC1 tail, we used luciferase reporters containing tandem repeats of TCF/LEF enhancer elements or mutated

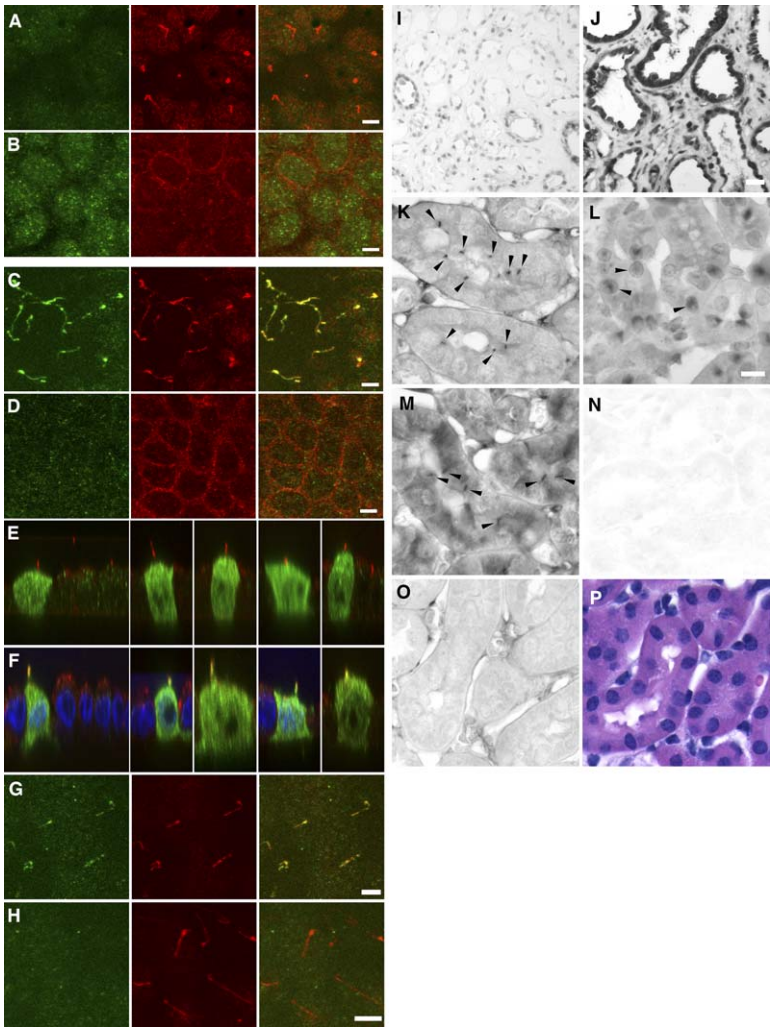

Figure 6. STAT6 Localizes to Cilia and Translocates to the Nucleus under "No-Flow" Conditions

(A–D) MDCK cells were cultured for 13 days on filter supports. Cells were then subjected to (C and D) orbital shaking at 1 Hz for 16 hr to mimic lumenal fluid flow or were (A and B) left unshaken. STAT6 (green) and tubulin (red) were detected by confocal immunofluorescence microscopy. The panels in (A) and (C) are projections of optical sections of the apical regions of the cells, whereas panels in (B) and (D) are projections of the nuclear regions of the same fields. The scale bar is 5 μm.

(E and F) MDCK cells were transiently transfected for V5-tagged STAT6 and were cultured for 24 hr on filter supports. Cells in (F) were subsequently shaken for 16 hr at 1 Hz, whereas cells in (E) were left unshaken. The confocal X-Z sections show immunostaining for acetylated tubulin (red), STAT6 (green), and nuclear DAPI staining (blue).

(G and H) MDCK cells were cultured and subjected to apical fluid flow as in (C) and (D). Cells were treated for 16 hr with (H) canine IL-4 or were (G) left untreated and stained for STAT6.

(I and J) Immunohistochemical detection of STAT6 in (J) ADPKD kidney or (I) normal human kidney. The scale bar is 20 μm.

(K–P) Analysis of mouse kidney. The kidney in (K), (M), and (O) was rapidly perfused with fixative, whereas the kidney in (L), (N), and (P) was fixed by immersion fixation. (K) and (L) are stained for STAT6. In (K), STAT6 is shown prominently localizing to primary cilia (arrowheads), whereas in (L), it is shown localizing to the nuclei. To detect primary cilia, the section in (M) was stained with an antibody against acetylated tubulin. (N) and (O) show negative controls with omission of the primary antibody. (P) shows an H&E-stained section. The scale bar is 10 μm.

elements (TOP- and FOP-FLASH, respectively). Neither the membrane-anchored nor any of the soluble PC1 constructs were able to stimulate β-catenin-dependent transcription (Figure 5F). Identical results were obtained by using a luciferase reporter construct containing the wnt-responsive *Siamois* promoter (data not shown). These results are consistent with a previous report of failure to affect wnt signaling by similar membrane-anchored PC1 constructs (Le et al., 2004) and suggest that PC1 and cleaved tail fragments may not be involved in the regulation of wnt signaling.

The FLM-PC1 and NTM-PC1 constructs have been reported to activate a signaling pathway resulting in increased AP-1-dependent transcription in HEK293 cells (Arnould et al., 1998). To test whether this may involve soluble fragments of the PC1 tail, we used an AP-1-responsive luciferase reporter. As shown in Figure 5G, the membrane-anchored FLM-PC1 and NTM-PC1 stimulate AP-1 activity as previously reported. However, all of the soluble PC1 tail constructs tested failed to stimulate AP-1 activity. These results indicate that not all signaling events involving the C terminus of PC1 require cleavage and nuclear translocation of the tail, and suggest that this is a specific function of the STAT6/P100-dependent pathway described here.

STAT6 Localizes to Cilia in Polarized MDCK Cells and Translocates to the Nucleus under "No-Flow" Conditions

The function of STAT6 in the immune system has been extensively investigated (Ostrand-Rosenberg et al., 2004). STAT6 is widely expressed in many other tissues, including the kidney (Hou et al., 1994; Quelle et al., 1995), but little is known about its function outside of the immune system. We tested where STAT6 may localize in polarized MDCK cells. Fully polarized MDCK cells exhibited nuclear localization of STAT6, but no immunosignal was detectable at the basal body or the primary cilia (Figures 6A and 6B). However, subjecting the cells to a constant flow of fluid across the apical membrane by culturing for 16 hr on an orbital shaker at 1 Hz caused a dramatic shift in the localization of STAT6. As shown in Figures 6C and 6D, a large fraction of STAT6 localizes to the primary cilia under these conditions with virtually no detectable nuclear signal. In order to ensure that the endogenous immunosignals are due to STAT6, we transiently transfected epitope-tagged STAT6 into MDCK cells and observed its localization. The cilia localization of transfected STAT6 responded exactly like endogenous STAT6 to the absence or presence of apical fluid flow (Figures 6E and 6F). Note that a large fraction of

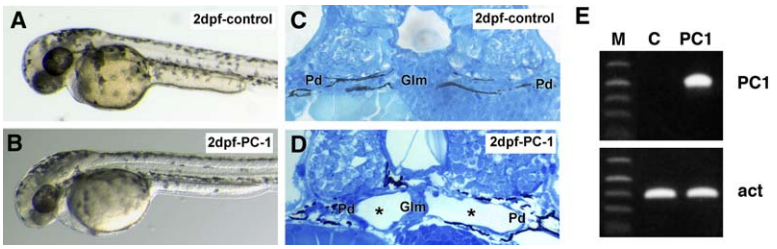

Figure 7. Expression of the Human PC1 Tail Causes Pronephric Cysts in Zebrafish Embryos

(A and B) Morphology of (A) control embryos and (B) embryos injected with 60 pg FLS-PC1 mRNA at 2 days postfertilization (dpf).

(C) Histology of a 2 dpf control embryo showing the glomerulus (Glm) and pronephric ducts (Pd).

(D) An FLS-PC1 mRNA-injected embryo showing cystic dilation of pronephric tubules (asterisks) and the glomerulus.

(E) RT-PCR analysis for human PC1 mRNA expression and β-actin in 3 dpf embryos. Control embryos (lane C) or human PC1-injected embryos (lane PC1) were analyzed with RT-PCR primers that generate a 522 bp product.

transiently transfected STAT6 localizes to the cytoplasm and nucleoplasm irregardless of apical fluid flow. This is likely due to the high overexpression level, and it suggests that primary cilia contain a limited and saturable number of STAT6 binding sites.

Treatment of "no-flow" MDCK cells with IL-4 for 30 min had no effect on STAT6 localization (data not shown). However, treatment of "flow" MDCK cells with IL-4 resulted in the loss of localization of STAT6 on cilia (Figures 6G and 6H), suggesting that tyrosine phosphorylation of STAT6 alone is sufficient for its translocation.

Together, these results suggest that STAT6 is involved in the transduction of a mechanical signal that originates at the primary cilia, and that this signal is activated under "no-flow" conditions.

Investigation of the expression and localization of STAT6 in human kidney revealed that STAT6 is moderately expressed in renal epithelial cells of normal control kidney (Figure 6I). In contrast, STAT6 is overexpressed in cyst-lining epithelial cells in ADPKD kidneys (Figure 6J), which was consistent among virtually all cysts in all patient specimens tested.

Since our available human "control" renal tissue specimens are normal adjacent tissues derived from nephrectomies due to renal tumors, the time lapse from the clamping of the renal artery during nephrectomy (which will halt renal tubular fluid flow) to the fixation of the tissue usually exceeds 1 hr. Furthermore, immersion fixation requires several hours to take full effect. Our above-described results with MDCK cells suggested that, under these conditions, STAT6 may have translocated from primary cilia to nuclei. In order to test whether the ciliary localization of STAT6 can be detected in rapidly fixed tissue, we perfused fixed mouse kidneys directly via the renal arteries. Surgical time was minimized to less than 3 min. Under these conditions, STAT6 is clearly detectable on primary cilia of renal epithelial cells (Figure 6K). In contrast, mouse kidneys fixed by conventional slow immersion fixation predominantly exhibited nuclear localization of STAT6 (Figure 6L) similar to human tissue (Figure 6I). Together, these results demonstrate that STAT6 translocates from primary cilia to the nuclei of renal epithelial cells in vitro and in vivo in response to the cessation of apical/lumenal fluid flow. Cysts in ADPKD kidneys exhibit very high nuclear expression of STAT6, indicating that STAT6-dependent gene expression is highly upregulated in ADPKD.

Expression of the PC1 Tail Causes Renal Cyst Formation in Zebrafish

We tested whether overexpression of the soluble PC1 tail alone may promote renal cyst formation. Zebrafish have been used extensively in the past as a model system by which to study renal cystogenesis (Drummond, 2005). Zebrafish embryos were injected at the one-cell stage with mRNA encoding the human PC1 tail (FLS-PC1). Control injected embryos show no morphological abnormalities during embryonic development (Figures 7A and 7C). In contrast, pronephric kidney cysts were observed histologically in PC1 tail mRNA-injected embryos examined at 2 days postfertilization (dpf) (Figure 7D). The pronephric kidney is the functional kidney of zebrafish embryos and larvae (Drummond et al., 1998). At 3 dpf, renal cysts and liver cysts were visible in 1098 (90%) of a total of 1220 injected embryos. This result indicates that exogenous overexpression of the soluble PC1 tail alone can recapitulate renal cyst formation in this model system.

Discussion

We demonstrate here a novel, to our knowledge, signaling mechanism by which PC1 regulates STAT6-dependent transcription. This involves cleavage of the cytoplasmic tail of PC1, which releases the C-terminal half of the tail from the membrane. This fragment binds to STAT6 and the transcriptional coactivator P100, translocates to the nucleus, and activates STAT6-dependent transcription. The finding that STAT6 translocates from cilia to nuclei in the absence of apical fluid flow makes it highly likely that this PC1/STAT6/P100 pathway is involved in the transduction of a mechanical signal to a transcriptional response. This pathway appears to be strongly upregulated in human ADPKD cysts, suggesting that it plays an important role in the pathogenesis of the human disease.

PC1 Tail Cleavage and Nuclear Translocation

Our finding of a nuclear immunosignal in renal epithelial cells with antibodies against the PC1 tail (Figure 1) is consistent with a recent report that demonstrated nuclear

PC1 in transgenic mice overexpressing PC1 (Chauvet et al., 2004). To our knowledge, for the first time, we report the nuclear localization of endogenous PC1 in human kidney and show that nuclear PC1 is highly upregulated in human ADPKD, which suggests that it plays a role in the disease process. Several investigators have reported cytoplasmic or membrane staining for PC1 in normal and ADPKD human kidney. While many of these reports have been in disagreement with each other with respect to the subcellular localization and cell type-specific expression, no nuclear localization has been reported (reviewed in Nauta et al., 2000). However, in many of these studies, antibodies against regions of PC1 other than the C-terminal tail were used with which no nuclear signal would be expected. Furthermore, histological nuclear counterstaining used in most studies would likely have obscured weak nuclear immunosignals. These are likely reasons why the nuclear localization of the PC1 tail has not, to our knowledge, previously been recognized.

The finding that the PC1 tail undergoes nuclear translocation after cleavage may place PC1 in a growing class of signaling membrane proteins that undergo "regulated intramembrane proteolysis" (RIP) (Urban and Freeman, 2002; Wolfe and Kopan, 2004). In most of these cases, the membrane protein is subjected to two proteolytic events. The first occurs in an extracytoplasmic domain and is followed by cleavage in a transmembrane domain that releases the cytoplasmic domain. It is intriguing that extracytoplasmic proteolysis at a GPS domain of PC1 has also been reported (Qian et al., 2002). In analogy to the situation, in most known cases of RIP, we speculate that GPS domain cleavage may precede the cleavage of the cytoplasmic tail.

Based on its molecular weight, we estimate that the cleavage site within the PC1 tail lies immediately N-terminal to the PEST sequence in the middle of the tail. In most examples of RIP, however, cleavage occurs within a transmembrane domain. We cannot exclude the possibility that PC1 first undergoes cleavage at a transmembrane domain, and that this is then followed by a secondary cleavage event, possibly by a soluble cytosolic protease. However, we observed that expression of the FLM-PC1 fusion protein also results in the generation of a fragment equivalent to the C-terminal half of the tail (Figure 2C). Since the transmembrane domain of FLM-PC1 is derived from a different protein (CD7), it appears unlikely that the same intramembrane proteolytic event would occur with this fusion protein. We therefore consider it more likely that the PC1 tail is cleaved by a membrane-associated or cytoplasmic protease that is not a typical RIP protease, but consists of a hydrophilic catalytic domain and cleaves a sequence in the middle of the tail. Chauvet et al. (2004) recently reported C-terminal cleavage of PC1 leading to the generation of a 34 kDa fragment that is considerably larger than the proteolytic product that we report here, and would be predicted to contain some of the last integral membrane domains of PC1. Although this remains to be tested, we speculate that this large fragment may be the product of a classical RIP protease such as γ-secretase. However, given the likely presence of hydrophobic domains, it appears unlikely that the 34 kDa fragment is the active component that undergoes nuclear translocation.

We show that the cleaved tail of PC1 is unstable and can only be detected after inhibition of proteasomal degradation. This is a common feature in most examples of RIP signaling (Urban and Freeman, 2002; Wolfe and Kopan, 2004). Our results suggest that a PEST sequence in the middle of the PC1 tail contributes to its rapid degradation. PEST domains are thought to mark proteins for degradation by the ubiquitin-proteasome pathway (Rechsteiner and Rogers, 1996). Interestingly, Kim et al. (2004) recently identified Siah-1 as an interacting protein to the C-terminal half of the PC1 tail and could show that this RING finger motif protein promotes the ubiquitin-dependent proteasomal degradation of PC1. Our results indicate that the PC1 tail is highly overexpressed in cyst-lining renal epithelial cells in ADPKD, where it exhibits significant nuclear localization. We therefore suggest that this phenotype may be caused either by enhanced cleavage of PC1 or by inhibition of its proteasomal degradation.

The Role of P100

P100 localizes to the basal body and primary cilia (Figure 4), and it interacts with the C-terminal half of the PC1 tail (Figure 3). This suggests that P100 may exist in a stable complex with PC1, which also partially localizes to cilia (Nauli et al., 2003; Yoder et al., 2002). P100 promotes cell growth (Tong et al., 1995). Given that we observed high expression of P100 in cysts, this suggests that it may be an important contributor to cyst formation and growth in ADPKD. We did not observe significant flow-induced differences of P100 localization in MDCK cells (data not shown). The reason for this may be that the expression level of P100 is much higher than that of STAT6 and PC1, and that P100 is likely to have many functions besides the STAT6/PC1 function described here. Interestingly, P100 has been shown to be strongly upregulated in mammary epithelial cells during lactation (Broadhurst and Wheeler, 2001). Under these conditions, mammary epithelial cells proliferate and undergo a differentiation program that results in a highly secretory phenotype. It is intriguing that proliferation and a change to a secretory phenotype are also hallmarks of affected renal epithelial cells in PKD.

The Role of STAT6

Expression of the PC1 tail resulted in stimulation of STAT6-dependent transcription, even in the absence of IL-4 stimulation. However, IL-4 treatment, which triggers tyrosine phosphorylation and dimerization of STAT6, strongly enhanced this effect. Furthermore, the STAT6-Y641F mutant was not stimulated by the PC1 tail. These results indicate that tyrosine-phosphorylated STAT6 is the active component in the PC1-regulated signaling pathway.

STAT proteins are tyrosine phosphorylated by members of the Janus kinase (JAK) family, tyrosine kinase growth factor receptors, nonreceptor tyrosine kinases, and seven transmembrane pass receptors (Calo et al., 2003). Four members of the JAK family are known: JAK1–3 and Tyk2. PC1 has previously been shown to bind to JAK2, which was shown to lead to activation of STAT1 (Bhunia et al., 2002). These authors did, however, not detect binding to JAK1 or Tyk2; JAK3 was not tested. In immune cells, STAT6 has been shown to be

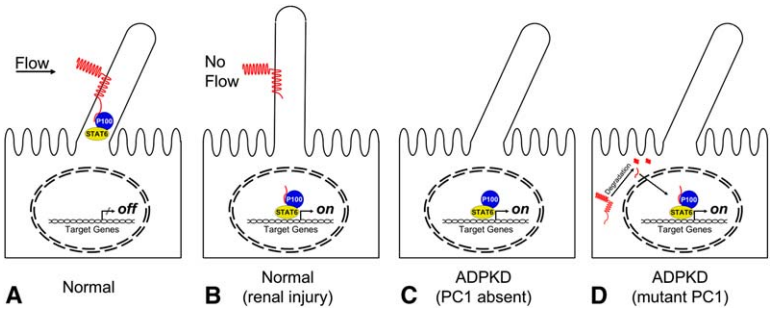

Figure 8. Model
(A–D) See Discussion for a description.

phosphorylated by JAK1 and JAK3, but not by JAK2. While this remains to be established, we propose that JAK3 may be involved in PC1-dependent activation of STAT6. Alternatively, JAK2 may exhibit altered substrate specificity when activated by PC1 and may be able to phosphorylate STAT6. Either way, PC1 is clearly a nonclassical activator of STAT function. Not only does it bind to a Janus kinase and cause tyrosine phosphorylation of STAT proteins (Bhunia et al., 2002), but it is also cleaved, and the resulting cytoplasmic fragment remains bound to the STAT protein to affect transcription in the nucleus as shown in this study. To our knowledge, this is the first example of such a mechanism of STAT activation.

Our results indicate that the function of the cleaved PC1 tail is specific to STAT6 activation and does not affect two other signaling pathways that have previously been shown to be affected by membrane-anchored fusion proteins containing the PC1 tail, namely, the wnt/β-catenin pathway and the AP-1 pathway. A recent report by Chauvet et al. (2004) appears to be inconsistent with our finding that AP-1 is unaffected. These authors report that a construct similar to our FLS-PC1 construct stimulates the response of an AP-1-sensitive luciferase reporter plasmid. However, Chauvet et al. (2004) did not observe AP-1 stimulation with a membrane-anchored fusion protein of the PC1 tail, which is in contrast to the results of three different groups (Arnould et al., 1998; Kim et al., 1999b; Le et al., 2004; Parnell et al., 2002) and to our findings (Figure 5G). Furthermore, Arnould et al. (1998) have previously reported that AP-1 activation depends on the membrane localization of the PC1 tail and is completely lost with a soluble PC1 construct that is similar to those used by us and Chauvet et al. Finally, the domain of PC1 that affects AP-1 signaling has been shown to be contained in the N-terminal half of the tail (Kim et al., 1999b), whereas our results show that the C-terminal half of the tail is released by proteolysis. Further work may be required to clarify this discrepancy.

Primary Cilia and Flow Sensing

We show that STAT6 is expressed in MDCK cells as well as in renal epithelial cells in vivo. In both cases, STAT6 localizes to the primary cilia under conditions of fluid flow across the apical plasma membrane. Mechanical stimulation of primary cilia in renal epithelial cells results in temporary elevation of cytosolic calcium (Nauli et al., 2003; Praetorius and Spring, 2001). It is likely that renal epithelial cells need to be able to respond quickly to changing rates of fluid flow. Whereas a calcium response is an ideal signal to affect fast and temporary cellular responses, we propose that STAT6-mediated signaling plays a role in a long-term response to changes in renal fluid flow. Renal injury may create conditions of ceased lumenal fluid flow, to which epithelial cells need respond by initiating a repair program that typically involves dedifferentiation and proliferation. In renal cystic diseases, lumenal fluid flow is strongly decreased or absent in dilated tubules and cysts, respectively. Our results suggest that, under these "no-flow" conditions, ciliary STAT6 will translocate to the nucleus and affect gene expression. The nuclear expression of STAT6, P100, and the cytoplasmic tail of PC1 are all highly elevated in cystic epithelial cells of ADPKD patients, which suggests that these cells may be in a state in which they inappropriately attempt to respond to a "no-flow" condition, such as that caused by renal injury. While the genes regulated by the PC1/STAT6/P100 pathway still need to be identified, we speculate that the activation of this pathway will trigger a proliferative response and a loss of differentiation, and that this is an important factor in renal cyst formation.

Model and Relevance to ADPKD

A working model that is consistent with our data is shown in Figure 8. Under normal flow conditions (Figure 8A), PC1 localizes to primary cilia, where it is in a complex with P100 and STAT6. The normal function of PC1 would be to sequester STAT6 and prevent the expression of STAT6/P100-dependent genes. This is supported by our finding that the membrane-anchored PC1 tail suppresses STAT6 activity (Figure 5D). This state remains stable as long as the cilia remain bent by lumenal fluid flow. Renal injury resulting in cessation of fluid flow (Figure 8B) will trigger cleavage of the cytoplasmic tail of PC1 by a yet unknown mechanism and protease. This is accompanied by STAT6 tyrosine phosphorylation, nuclear translocation of the PC1 tail/STAT6/P100 complex, and activation of gene expression.

We propose two scenarios that will lead to aberrant STAT6 activity in ADPKD. If PC1 is completely lost (e.g., due to a large gene deletion in both alleles, an unlikely event), STAT6 cannot be sequestered at the cilia and may be constitutively activated (Figure 8C). This scenario should also apply to PKD1 knockout mouse models. It is more commonly observed in ADPKD that PC1 is actually highly expressed in cyst-lining epithelial cells. However, overexpressed mutant PC1 may be misfolded and degraded. Degradation of PC1 may release

a biologically active fragment corresponding to the C-terminal half of the tail. In this scenario (Figure 8D), not only would STAT6 fail to be sequestered at the cilia, but the PC1 tail would further increase STAT6-dependent transcription. This scenario is consistent with our finding of high levels of nuclear PC1 tail in ADPKD cysts.

Similarly, mutations in other genes whose products are required for cilia formation or function may also interfere with the inhibitory action of PC1 on STAT6 transcription. Consistent with this model, the products of most genes that have been identified in animal models of renal cystic diseases have been shown to localize to primary cilia (Delmas, 2004; Guay-Woodford, 2003; Zhang et al., 2004).

Our model predicts that a loss of STAT6 function, per se, may have little effect in a normal kidney. Indeed, STAT6 null mice have been generated, and there has been no report of any severe renal phenotype. Almost the entire research effort to elucidate STAT6 function has been focused on the immune system despite the fact that this protein is widely expressed, including in the kidney, as demonstrated previously by Northern blot analysis (Hou et al., 1994) and as shown in this study.

It is striking that expression of the soluble PC1 tail alone results in renal cyst formation in zebrafish. This suggests that the function of the soluble PC1 tail is highly conserved in evolution. Zebrafish have proteins closely related to human P100 (Broadhurst et al., 2005) and STAT6 (our unpublished data), but it remains to be investigated whether they function in a common pathway.

Overall, our results suggest that the PC1/STAT6/P100 signaling pathway described here plays an important role in the cellular response to tubular fluid flow, and that it is an important regulator of renal cyst formation in ADPKD. Components of this pathway may be promising targets for novel therapeutic approaches for the treatment of ADPKD.

Experimental Procedures

Plasmids

cDNAs of membrane-anchored PC1 constructs were gifts from Gerd Walz (University Hospital Freiburg) and were cloned into pCDNA4/TO (Invitrogen). All other PC1 constructs were made by PCR and cloning into pCDNA4/TO-myc-His (Invitrogen). Two aspartate residues in the PEST sequence (residues 4173 and 4182) were replaced by alanines in CTSP- and FLS-PC1. FLAG-tagged PC1 was provided by Gregory Germino (Johns Hopkins University). A STAT6-luciferase reporter containing five copies of a STAT6 binding element (N_6-GAS) (Haque et al., 1997) and plasmids encoding human STAT6 and V5-tagged STAT6 were provided by Saikh Jaharul Haque and Pankaj Sharma (Cleveland Clinic). A luciferase reporter containing AP-1 response elements $(TGACTAA)_7$ was obtained from Stratagene. A constitutively active HA-tagged β-catenin (S37A) mutant and Siamois promoter-Luciferase constructs were gifts from Catherine Mao (University of Kentucky) and Randall Moon (University of Washington), respectively. TOP- and FOP-FLASH reporter plasmids were provided by Philip Howe and Barbara Hocevar (Cleveland Clinic).

Antibodies

Rabbit polyclonal antibodies (αFL and αCT) against the PC1 tail were generated against GST fusion proteins corresponding to the FLS or CTS constructs. Antibodies were affinity purified by using the antigen cleaved from GST by thrombin and were immobilized on Affigel (BioRad). Polyclonal antibodies against a C-terminal 16 kDa fragment or an N-terminal 43 kDa fragment of P100 (Broadhurst and Wheeler, 2001) were provided by Tom Wheeler (AgResearch, Hamilton, New Zealand). An additional polyclonal rabbit P100 antibody was generated by using a full-length P100-GST fusion protein as described above.

Luciferase Assays

A total of 10^6 HEK293T cells were cultured overnight in six-well plates to 80% confluency and were transfected with 3 μg luciferase reporter and 150 ng β-galactosidase plasmid per well by using Lipofectamine2000 (Invitrogen). Four hours posttransfection an equal volume of media containing 20% FBS was added. After 16–18 hr, cells were spilt into 12-well plates, and 6 hr later, they were induced with IL-4 (R&D Systems). GFP in pCDNA4/TO was used for balancing the plasmids in all transfections. Luciferase assays were carried out after 16 hr of treatment with IL-4 with luciferase substrate (Promega), and β-gal was detected by using ONPG in sodium phosphate buffer.

Immunofluorescence

MDCK cells were allowed to polarize by plating 0.5 million cells onto Transwell filters, and cells were grown for 10–13 days. Prior to immunofluorescence staining, cells were rotated on an orbital shaker overnight at 1 Hz as described previously (Kolb et al., 2004). Nonpolarized MDCK cells for transfection were plated on coverslips and were transfected while in suspension and incubated overnight before staining. Immunostaining was carried out as described previously (Weimbs et al., 2003).

Immunoprecipitation

Cells were washed in cold PBS and scraped with lysis buffer (50 mM HEPES KOH [pH 7.4], 50 mM K-acetate, and 1% Triton X-100) containing protease inhibitor cocktail, phosphatase inhibitors, and 0.5% BSA, and they were rotated for 30 min at 4ºC. Precleared lysates were used for immunoprecipitation with anti-STAT6 antibody (Santa Cruz, Inc., CA) overnight at 4ºC and were subsequently pulled down by using protein A Sepharose beads for 1 hr at 4ºC. The beads were washed with lysis buffer three times. Samples were analyzed by Western blotting with the indicated antibodies.

Cell Fractionation

MDCK cells cultured on 10 cm dishes were rinsed with ice-cold PBS, were scraped into 0.5 ml hypotonic buffer (20 mM HEPES, 5 mM EDTA, protease inhibitors), and were passed through a 25 gauge needle to break the cells. A 1,000 × g spin was performed for 2 min at 4ºC to pellet the nuclei, and the supernatant was spun at 16,000 × g for 30 min at 4ºC to pellet the membranes. The fractions were loaded onto SDS-PAGE gels, and a Western blot was performed with the antibodies indicated in the figure legends.

Human Samples

Tissue samples from ADPKD patients and normal controls were obtained at the Cleveland Clinic as per institutional guidelines. Samples were fixed and embedded in paraffin for immunohistochemistry.

Zebrafish Experiments

Wild-type AB zebrafish were maintained and raised as described (Westerfield, 1993). Zebrafish embryos were kept at 28.5ºC in E3 solution and were staged according to hours postfertilization (hpf). Embryos were microinjected at the one-cell stage with 20–60 pg capped mRNA encoding FLS-PC1. In vitro-transcribed mRNA was synthesized by using a mMessage mMachine T7 kit (Ambion) and was injected into 200 mM KCl, 0.1% phenol red. Nested PCR primers were used to detect human PC1 to confirm the expression in the injected zebrafish embryos. Amplification of β-actin was performed as a positive control. Embryos were fixed in 1.5% glutaraldehyde, 1% paraformaldehyde, 70 mM NaPO4 (pH 7.2), 3% sucrose overnight at 4ºC and were embedded in JB-4 resin (Polysciences) and sectioned at 3 μm with HM325 (Richard-Allan Scientific). Slides were stained with Methylene Blue and Azure II as described before (Drummond et al., 1998).

Identification of P100 as a PC1 Binding Protein

MDCK cells stably expressing the CTM-PC1 construct were cultured to confluency on 10 cm dishes. The cells were untreated (control) or induced with 50 ng/ml DOX for 16 hr. Cells were lysed in 50 mM HEPES, 50 mM K-acetate, 2% Triton X-100, protease inhibitors.

CTM-PC1 was immunoprecipitated with protein A Sepharose coupled to anti-CD16 antibody (Becton Dickson, CA). The beads were washed with the above-described buffer, and bound proteins were analyzed by SDS-PAGE. Coomassie blue-stained, specific bands were excised, washed with 50% ethanol/5% acetic acid, reduced with DTT, alkylated with iodoacetamide, and digested with trypsin (Kinter and Sherman, 2000). The digests were analyzed by capillary column LC-tandem mass spectrometry on a ThermoFinnigan LCQdeca ion trap system with a nanospray ion source. Mass spectra and CID spectra were collected, and CID spectra were used to search the NCBI nonredundant database. All matching spectra were verified by manual interpretation.

GST-P100 Binding Assay

MDCK cells stably transfected with CTM-PC1 were uninduced or induced with 50 ng/ml DOX for 16 hr. The cells were lysed in 50 mM HEPES (pH 7.4), 150 mM K-acetate, 2 mM DTT, 2% TX-100, protease inhibitors. Precleared lysates were incubated with GST or GST-P100 fusion proteins immobilized on glutathione Sepharose beads (Amersham) for 4 hr at 4ºC. Beads were washed four times with lysis buffer, and proteins were analyzed by SDS-PAGE and immunoblotting.

Acknowledgments

We are grateful to Gregory Germino, Saikh Jaharul Haque, Barbara Hocevar, Philip Howe, Catherine Mao, Randall Moon, Richard Morton, Pankaj Sharma, George Stark, Gerd Walz, and Tom Wheeler for generous gifts of reagents and helpful discussions. We thank Ryan Hedgepeth, Xin Li, Noel Murcia, Jonathan Shillingford, Frances Stedham, and Johan Waern for help with experiments. This work was supported by grants from the National Institutes of Health to T.W. (R01-DK62338) and T.O. (R21-DK069604-01), a Scientist Development Grant from the American Heart Association to S.H.L, and by the generous support of Martha and Jerry Jarrett to T.W.

Received: January 6, 2005
Revised: June 15, 2005
Accepted: December 8, 2005
Published: January 9, 2006

References

Arnould, T., Kim, E., Tsiokas, L., Jochimsen, F., Gruning, W., Chang, J.D., and Walz, G. (1998). The polycystic kidney disease 1 gene product mediates protein kinase C α-dependent and c-Jun N-terminal kinase-dependent activation of the transcription factor AP-1. J. Biol. Chem. *273*, 6013–6018.

Bhunia, A.K., Piontek, K., Boletta, A., Liu, L., Qian, F., Xu, P.N., Germino, F.J., and Germino, G.G. (2002). PKD1 induces p21(waf1) and regulation of the cell cycle via direct activation of the JAK-STAT signaling pathway in a process requiring PKD2. Cell *109*, 157–168.

Broadhurst, M.K., and Wheeler, T.T. (2001). The p100 coactivator is present in the nuclei of mammary epithelial cells and its abundance is increased in response to prolactin in culture and in mammary tissue during lactation. J. Endocrinol. *171*, 329–337.

Broadhurst, M.K., Lee, R.S., Hawkins, S., and Wheeler, T.T. (2005). The p100 EBNA-2 coactivator: a highly conserved protein found in a range of exocrine and endocrine cells and tissues in cattle. Biochim. Biophys. Acta *1681*, 126–133.

Calo, V., Migliavacca, M., Bazan, V., Macaluso, M., Buscemi, M., Gebbia, N., and Russo, A. (2003). STAT proteins: from normal control of cellular events to tumorigenesis. J. Cell. Physiol. *197*, 157–168.

Chauvet, V., Tian, X., Husson, H., Grimm, D.H., Wang, T., Hieseberger, T., Igarashi, P., Bennett, A.M., Ibraghimov-Beskrovnaya, O., Somlo, S., and Caplan, M.J. (2004). Mechanical stimuli induce cleavage and nuclear translocation of the polycystin-1 C terminus. J. Clin. Invest. *114*, 1433–1443.

Delmas, P. (2004). Polycystins: from mechanosensation to gene regulation. Cell *118*, 145–148.

Drummond, I.A. (2005). Kidney development and disease in the zebrafish. J. Am. Soc. Nephrol. *16*, 299–304.

Drummond, I.A., Majumdar, A., Hentschel, H., Elger, M., Solnica-Krezel, L., Schier, A.F., Neuhauss, S.C., Stemple, D.L., Zwartkruis, F., Rangini, Z., et al. (1998). Early development of the zebrafish pronephros and analysis of mutations affecting pronephric function. Development *125*, 4655–4667.

Guay-Woodford, L.M. (2003). Murine models of polycystic kidney disease: molecular and therapeutic insights. Am. J. Physiol. Renal Physiol. *285*, F1034–F1049.

Haque, S.J., Wu, Q., Kammer, W., Friedrich, K., Smith, J.M., Kerr, I.M., Stark, G.R., and Williams, B.R. (1997). Receptor-associated constitutive protein tyrosine phosphatase activity controls the kinase function of JAK1. Proc. Natl. Acad. Sci. USA *94*, 8563–8568.

Hou, J., Schindler, U., Henzel, W.J., Ho, T.C., Brasseur, M., and McKnight, S.L. (1994). An interleukin-4-induced transcription factor: IL-4 Stat. Science *265*, 1701–1706.

Igarashi, P., and Somlo, S. (2002). Genetics and pathogenesis of polycystic kidney disease. J. Am. Soc. Nephrol. *13*, 2384–2398.

Kim, E., Arnould, T., Sellin, L., Benzing, T., Comella, N., Kocher, O., Tsiokas, L., Sukhatme, V.P., and Walz, G. (1999a). Interaction between RGS7 and polycystin. Proc. Natl. Acad. Sci. USA *96*, 6371–6376.

Kim, E., Arnould, T., Sellin, L.K., Benzing, T., Fan, M.J., Gruning, W., Sokol, S.Y., Drummond, I., and Walz, G. (1999b). The polycystic kidney disease 1 gene product modulates Wnt signaling. J. Biol. Chem. *274*, 4947–4953.

Kim, H., Jeong, W., Ahn, K., Ahn, C., and Kang, S. (2004). Siah-1 interacts with the intracellular region of polycystin-1 and affects its stability via the ubiquitin-proteasome pathway. J. Am. Soc. Nephrol. *15*, 2042–2049.

Kinter, M., and Sherman, N.E. (2000). Protein Sequencing and Identification Using Tandem Mass Spectrometry (New York: John Wiley and Sons, Inc.).

Kolb, R.J., Woost, P.G., and Hopfer, U. (2004). Membrane trafficking of angiotensin receptor type-1 and mechanochemical signal transduction in proximal tubule cells. Hypertension *44*, 352–359.

Le, N.H., Van Der Bent, P., Huls, G., Van De Wetering, M., Loghman-Adham, M., Ong, A.C., Calvet, J.P., Clevers, H., Breuning, M.H., Van Dam, H., and Peters, D.J. (2004). Aberrant polycystin-1 expression results in modification of AP-1 activity, while Wnt signaling remains unaffected. J. Biol. Chem. *279*, 27472–27481.

Nauli, S.M., and Zhou, J. (2004). Polycystins and mechanosensation in renal and nodal cilia. Bioessays *26*, 844–856.

Nauli, S.M., Alenghat, F.J., Luo, Y., Williams, E., Vassilev, P., Li, X., Elia, A.E., Lu, W., Brown, E.M., Quinn, S.J., et al. (2003). Polycystins 1 and 2 mediate mechanosensation in the primary cilium of kidney cells. Nat. Genet. *33*, 129–137.

Nauta, J., Goedbloed, M.A., van den Ouweland, A.M., Nellist, M., and Hoogeveen, A.T. (2000). Immunological detection of polycystin-1 in human kidney. Histochem. Cell Biol. *113*, 303–311.

Ostrand-Rosenberg, S., Sinha, P., Clements, V., Dissanayake, S.I., Miller, S., Davis, C., and Danna, E. (2004). Signal transducer and activator of transcription 6 (Stat6) and CD1: inhibitors of immunosurveillance against primary tumors and metastatic disease. Cancer Immunol. Immunother. *53*, 86–91.

Parnell, S.C., Magenheimer, B.S., Maser, R.L., Rankin, C.A., Smine, A., Okamoto, T., and Calvet, J.P. (1998). The polycystic kidney disease-1 protein, polycystin-1, binds and activates heterotrimeric G-proteins in vitro. Biochem. Biophys. Res. Commun. *251*, 625–631.

Parnell, S.C., Magenheimer, B.S., Maser, R.L., Zien, C.A., Frischauf, A.M., and Calvet, J.P. (2002). Polycystin-1 activation of c-Jun N-terminal kinase and AP-1 is mediated by heterotrimeric G proteins. J. Biol. Chem. *277*, 19566–19572.

Praetorius, H.A., and Spring, K.R. (2001). Bending the MDCK cell primary cilium increases intracellular calcium. J. Membr. Biol. *184*, 71–79.

Praetorius, H.A., and Spring, K.R. (2003). The renal cell primary cilium functions as a flow sensor. Curr. Opin. Nephrol. Hypertens. *12*, 517–520.

Qian, F., Boletta, A., Bhunia, A.K., Xu, H., Liu, L., Ahrabi, A.K., Watnick, T.J., Zhou, F., and Germino, G.G. (2002). Cleavage of

polycystin-1 requires the receptor for egg jelly domain and is disrupted by human autosomal-dominant polycystic kidney disease 1-associated mutations. Proc. Natl. Acad. Sci. USA *99*, 16981–16986.

Quelle, F.W., Shimoda, K., Thierfelder, W., Fischer, C., Kim, A., Ruben, S.M., Cleveland, J.L., Pierce, J.H., Keegan, A.D., Nelms, K., et al. (1995). Cloning of murine Stat6 and human Stat6, Stat proteins that are tyrosine phosphorylated in responses to IL-4 and IL-3 but are not required for mitogenesis. Mol. Cell. Biol. *15*, 3336–3343.

Rechsteiner, M., and Rogers, S.W. (1996). PEST sequences and regulation by proteolysis. Trends Biochem. Sci. *21*, 7267–7271.

Sutters, M., and Germino, G.G. (2003). Autosomal dominant polycystic kidney disease: molecular genetics and pathophysiology. J. Lab. Clin. Med. *141*, 91–101.

Tong, X., Drapkin, R., Yalamanchili, R., Mosialos, G., and Kieff, E. (1995). The Epstein-Barr virus nuclear protein 2 acidic domain forms a complex with a novel cellular coactivator that can interact with TFIIE. Mol. Cell. Biol. *15*, 4735–4744.

Torres, V.E., and Harris, P.C. (2003). Autosomal dominant polycystic kidney disease. Nefrologia *23* (*Suppl 1*), 14–22.

Urban, S., and Freeman, M. (2002). Intramembrane proteolysis controls diverse signalling pathways throughout evolution. Curr. Opin. Genet. Dev. *12*, 512–518.

Vandorpe, D.H., Chernova, M.N., Jiang, L., Sellin, L.K., Wilhelm, S., Stuart-Tilley, A.K., Walz, G., and Alper, S.L. (2001). The cytoplasmic carboxy-terminal fragment of polycystin-1 (PKD1) regulates a Ca{super2}+-permeable cation channel. J. Biol. Chem. *23*, 4093–4101.

Weimbs, T., Low, S.H., Li, X., and Kreitzer, G. (2003). SNAREs and epithelial cells. Methods *30*, 191–197.

Westerfield, M. (1993). The Zebrafish Book: A Guide for the Laboratory Use of Zebrafish (*Brachydanio rerio*) (Eugene, OR: The University of Oregon Press).

Wilson, P.D. (2004). Polycystic kidney disease. N. Engl. J. Med. *350*, 151–164.

Wolfe, M.S., and Kopan, R. (2004). Intramembrane proteolysis: theme and variations. Science *305*, 1119–1123.

Xu, G.M., Gonzalez-Perrett, S., Essafi, M., Timpanaro, G.A., Montalbetti, N., Arnaout, M.A., and Cantiello, H.F. (2003). Polycystin-1 activates and stabilizes the polycystin-2 channel. J. Biol. Chem. *278*, 1457–1462.

Yang, J., Aittomaki, S., Pesu, M., Carter, K., Saarinen, J., Kalkkinen, N., Kieff, E., and Silvennoinen, O. (2002). Identification of p100 as a coactivator for STAT6 that bridges STAT6 with RNA polymerase II. EMBO J. *21*, 4950–4958.

Yoder, B.K., Hou, X., and Guay-Woodford, L.M. (2002). The polycystic kidney disease proteins, polycystin-1, polycystin-2, polaris, and cystin, are co-localized in renal cilia. J. Am. Soc. Nephrol. *13*, 2508–2516.

Zhang, Q., Taulman, P.D., and Yoder, B.K. (2004). Cystic kidney diseases: all roads lead to the cilium. Physiology (Bethesda) *19*, 225–230.